PHYSICAL REVIEW B VOLUME 46, NUMBER 14 1 OCTOBER 1992-II

Temperature dependence of the infrared and optical properties of *N*-dimethyl thiomorpholinium(tetracyanoquinodimethane)$_2$

J. L. Musfeldt
Department of Chemistry, University of Florida, Gainesville, Florida 32611

C. C. Homes
Department of Physics and Astronomy, McMaster University, Hamilton, Ontario, Canada L8S 4M1

M. Almeida
Departamento de Química, Instituto de Ciências e Engenharia Nucleares, Laboratório Nacional de Engenharia e Tecnologia Industrial, P2686 Sacavem Codex, Portugal

D. B. Tanner
Department of Physics, University of Florida, Gainesville, Florida 32611
(Received 18 May 1992)

We report the infrared and optical reflectance spectrum of semiconducting *N*-dimethyl thiomorpholinium (tetracyanoquinodimethane)$_2$ at temperatures above and below the structural phase transition. Polarized measurements were made on several faces of large single crystal samples. For polarization close to the tetracyanoquinodimethane (TCNQ) stacking axis, the spectrum resembles other many weakly conducting TCNQ salts, with strong vibrational features and two charge-transfer bands. The infrared data in this polarization were analyzed within the framework of both an isolated dimer model and a twofold-commensurate charge-density-wave model. We have obtained experimental values of the unperturbed phonon frequencies and linear electron-molecular-vibration coupling constants, both of which are nearly independent of temperature. The dimer model fails to reproduce the phonon intensities and line shapes and underestimates the coupling constants, whereas the charge-density-wave model produces better results in both cases. We have also investigated whether the structural phase transition leads to a change of electronic structure (because of crystal-field distortion) that can account for the observed dc conductivity. For light polarized close to the *b* crystallographic axis, the spectral data are, overall, not in good agreement with the proposed band structure. In the low-temperature phase, several expected low-energy excitations are absent, most notably the low-energy interband expected near 430 cm^{-1}. In the absence of spectral evidence for this low-energy transition, the activation energy for interchain transport is $\approx$0.25 eV both above and below T_c. Consequently, our data do not support the idea that the unusual transport properties of semiconducting DMTM(TCNQ)$_2$ are caused by low-energy interchain charge transfer.

I. INTRODUCTION

N-N'-dimethyl-thiomorpholinium bis-7,7',8,8'-tetracyanoquinodimethane, [DMT(TCNQ)$_2$] is a "quarter-filled" semiconducting organic charge-transfer salt containing segregated chains of TCNQ dimers and DMTM counterions. This material undergoes a first order structural phase transition at a critical temperature (T_c) of 272 K, with the unusual feature that the dc conductivity is three orders of magnitude *higher* below the transition temperature.[1] More specifically, $\sigma_{dc}=10^{-2}$ Ω^{-1} cm^{-1} and $E_A=0.26$ eV just above the phase transition; $\sigma_{dc}=3$ Ω^{-1} cm^{-1} and $E_A=0.03$ eV just below it.[1,2] This unusual behavior (shown in Fig. 1) has been described as an "inverted Peierls transition," and has tentatively been explained in terms of a crystal-field distortion.[3]

Structural studies[3-5] reveal that the high-temperature phase is monoclinic, with the TCNQ molecules stacked in a dimerized fashion along the *c* direction. The intradimer and interdimer distances are 3.25 and 3.29 Å, respectively. The DMTM cations, which are located on mirror planes, are disordered. The mirror planes result in the crystallographic equivalence of the two TCNQ sheets (as defined by the *a*/*c* plane) within the unit cell.

In the low-temperature phase, the crystal symmetry is reduced to a triclinic space group. At T_c, the *b* axis rotates slightly (about 10° away from the normal) into the *a*/*c* plane. It is likely that ordering of the DMTM counterions results in the loss of the mirror plane symmetry. The reduced crystal symmetry results in the crystallographic inequivalence of the two TCNQ sheets within the unit cell. The structure of the two TCNQ sheets in the unit cell (defined by the *a*/*c* plane) is unaffected by the phase transition.

The unusual transport properties of DMTM(TCNQ)$_2$ have tentatively been explained in terms of a crystal-field distortion.[3] The band structure which is thought to re-

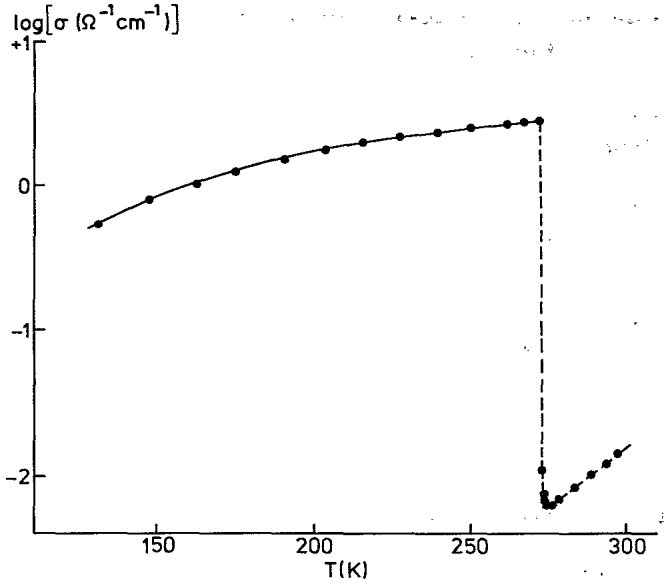

FIG. 1. Logarithm of dc conductivity vs temperature along c^* for DMTM(TCNQ)$_2$, indicating a first-order phase transition at $T_c \approx 272$ K.

sult from this distortion is diagramed in Fig. 2. The proposed band structure of quarter-filled DMTM(TCNQ)$_2$ in the high-temperature phase (monoclinic) is shown on the left. A crystal-field distortion along the b axis at the phase transition temperature reduces the crystal symmetry (to triclinic), causing a splitting of the bands, as shown on the right. Four other bands in a similar configuration are at higher energy, separated from those shown in Fig. 2 by the Hubbard gap.

In terms of transport, the net effect of the distortion is to reduce the energy gap between the valence and conduction bands. Based upon this argument, one would predict a large decrease in the activation energy for transport in the low-temperature phase, thus facilitating thermal excitation of the carriers. Indeed, the activation energy for conduction (E_A) has been measured to be 0.26 and 0.03 eV in the high- and low-temperature phases, respectively.[1,2] In the high-temperature phase, the small value of the dc conductivity and the large value of the activation energy suggests that the dc conductivity is due to hopping.[6,7] Despite the "inverted Peierls" nature of the low-temperature phase, the dc conductivity is relatively low, suggesting both a modest number of carriers and a limited mobility.

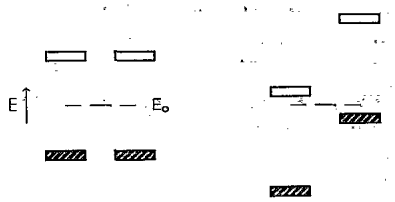

FIG. 2. Band-structure modifications of the proposed crystal-field distortion, which occurs in the b crystallographic direction.

Thermopower measurements[2] on DMTM(TCNQ)$_2$ also show clear evidence of a first-order structural phase transition, in agreement with previous results. In the low-temperature phase, these data are consistent with that expected for a transition to a small band-gap semiconductor with a gap of 0.06 eV. Thus, thermopower provides further evidence for a reduction of the band gap at T_c, in support of the crystal-field distortion theory by Visser *et al.*[3]

Magnetic-susceptibility (χ) measurements[1] display the inverted Peierls behavior as well. In the high-temperature phase, χ rises slightly from its room-temperature value of $\approx 1.0\times10^{-3}$ emu/mol. At T_c, χ drops sharply from a value of $\approx 1.2\times10^{-3}$ to $\approx 1.0\times10^{-3}$ emu/mol and then rises with a further decrease in temperature to a value of 2.2×10^{-3} emu/mol; below 50 K, χ drops sharply, reminiscent of a spin-Peierls transition. From an extrapolation of these results to zero temperature, it has been suggested that the value of χ may be consistent with two different TCNQ chains in the low-temperature phase, possibly one with and one without a $2k_F$ distortion.

High-resolution ^{13}C NMR studies[8,9] on DMTM(TCNQ)$_2$ show unusually large chemical shifts of lines assigned to CN groups. Below T_c, these lines split due to the inequivalence of the two TCNQ molecules in the unit cell. Because of the unusually large chemical shift of these lines, it is suggested that they are Knight shifts, and thus related to the unpaired electron density on the dimer. The Knight shift increases with decreasing temperature, in accord with the magnetic-susceptibility measurements.

Electron paramagnetic resonance (EPR) studies on single-crystal samples[10] also confirm the inequivalence of the TCNQ chains below the phase-transition temperature as proposed by the crystal-field distortion model.

In order to provide further information on the nature of the high- and low-temperature phases, we have investigated the infrared and optical properties of DMTM(TCNQ)$_2$. Spectroscopic methods are well suited to the study of highly anisotropic materials such as the TCNQ charge-transfer salts, providing information on the electronic charge transfer and localized excitations at high energies, as well as the vibrational features and electron-phonon coupling at lower energies.[11–14] Our results, and in particular the electron-phonon coupling in the chain direction, have been treated within the framework of a molecular cluster model for an isolated dimer by Rice, Yartsev, and Jacobsen[15] and a model for commensurate charge-density waves in extended linear chains initially devised by Rice[16] and developed into the current model by Bozio, Meneghetti, and Pecile.[17] In both of these models, the totally symmetric A_g modes of the TCNQ molecule, normally infrared inactive, become optically active through a charge-transfer process, and show unusually large oscillator strengths. Emphasis has been placed on the correlation of the spectral properties above and below T_c with available structural and transport data as well as the band structure proposed by Visser *et al.*,[3] with the goal of obtaining a greater understanding of the

characteristics and mechanism of the structural phase transition.

We will also compare our results for $DMTM(TCNQ)_2$ with the well-studied *N*-methyl-*N*-ethyl morpholinium $(TCNQ)_2$ [$MEM(TCNQ)_2$] system.[15,18–20] The counterions in these two materials are closely related, the most notable difference being the more polarizable sulfur atom on the DMTM ring.

II. EXPERIMENT

$DMTM(TCNQ)_2$ was prepared by the reaction of TCNQ with the cation iodide in boiling acetonitrile under a nitrogen atmosphere. Large single crystals, up to $\approx 5\times5\times1.5$ mm^3, were grown by slow cooling of deaerated saturated and seeded solutions under dry nitrogen, using a technique similar to that previously described for other complex TCNQ salts.[21,22]

Near-normal polarized reflectance measurements were made on unique faces of single-crystal samples of $DMTM(TCNQ)_2$. Figure 3 depicts the typical crystal shape and labels the crystallographic faces of $DMTM(TCNQ)_2$. Note that the a/c plane defines the (010) face of the sample. In this paper, we report our measurements on the (010) and (110) faces.

Experiments were performed with light polarized parallel and perpendicular to the maximum reflectance on each unique crystal face. Symmetry requires that two of the principal axes of the high-temperature phase lie on the (010) face. Once the optic axes were found at 300 K, the polarizer position remained unchanged for all temperatures studied.

For each polarization, infrared measurements (40–5000 cm^{-1}) were made at five temperatures from 60 to 300 K, concentrated around T_c (272 K). In the near-infrared region (4000–15 000 cm^{-1}), data were collected at $\approx$100 and 300 K. Reflectance measurements for the visible frequency region (15 000–30 000 cm^{-1}) were collected at room temperature. Our experimental apparatus for the near-infrared, visible, and near-ultraviolet measurements has been described in detail elsewhere.[23] The total frequency range of data collection ran from 40 to 30 000 cm^{-1}.

Due to the wide frequency range of our measurements, the optical constants can be obtained by Kramers-Kronig analysis[24] of the power reflectance spectrum. This analysis allows the complex dielectric function

$$\tilde{\epsilon}(\omega)=\epsilon_1(\omega)+i\epsilon_2(\omega)=\epsilon_1(\omega)+\frac{4\pi i}{\omega}\sigma_1(\omega) \quad (1)$$

to be calculated. Here, ϵ_1 is the real part of the dielectric function and σ_1 is the frequency-dependent conductivity. The low-frequency data were extrapolated to zero frequency assuming a constant reflectance, a common procedure for semiconducting materials. The high-frequency data were extended as ω^{-4} to simulate free-electron behavior. Under a microscope, the samples were smooth, so no attempt was made to coat the surface with aluminum to correct for scattering loss.

III. RESULTS

A. (010) crystal face

1. Room-temperature spectra

a. Parallel to R_{max}. Figure 4 shows the room-temperature reflectance on the (010) face over the entire spectral range for polarizations parallel and perpendicular to the direction of maximum reflectance (R_{max}). Assuming that two principal axes are located in this plane, the R_{max} direction (and thus, the direction perpendicular to R_{max}) must be those principal axes of the crystal. No clear evidence of a change in the R_{max} direction with wavelength was found (except for the trivial exchange by 90° between 6000 and 18 000 cm^{-1}), although the crystal symmetry allows for such dispersion.

For the electric-field vector polarized along R_{max}, the spectrum display two electronic excitations ($\approx$3200 and $\approx$10 500 cm^{-1}); the mid-infrared band contains a majority of the oscillator strength. In other strongly dimerized TCNQ salts these absorptions have been attributed to the

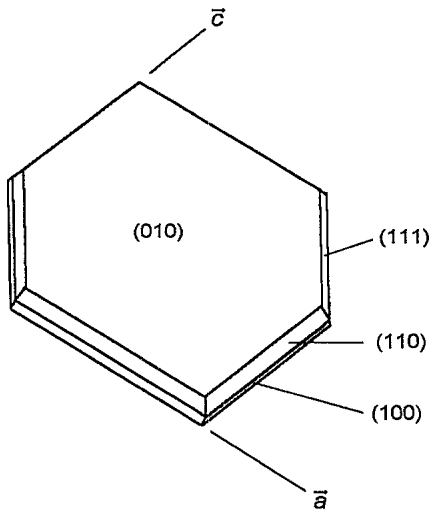

FIG. 3. Diagram of $DMTM(TCNQ)_2$ single-crystal facets.

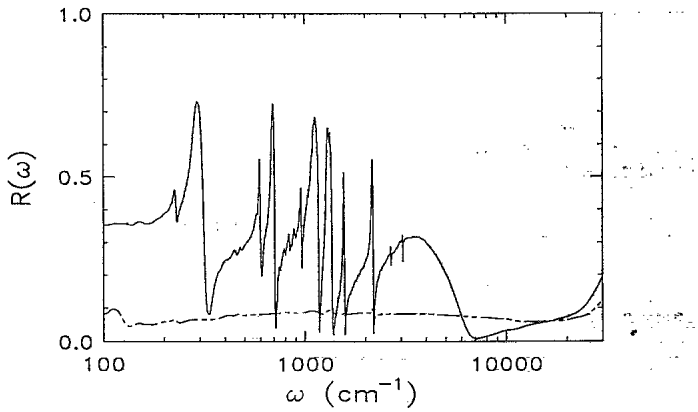

FIG. 4. Room-temperature reflectance of $DMTM(TCNQ)_2$, with light polarized along the maximum reflectance direction (solid line) and perpendicular (dashed line) to it on the large (010) crystal face.

transfer of charge between TCNQ molecules in the stack.[15,25,26] At low frequency, the spectra display many sharp vibrational features. Ten of these modes are A_g vibrations of the TCNQ molecule, activated by coupling to the charge-transfer excitations.[15,16] The presence of these well-known features[27,28] in this polarization indicates that R_{max} is in the direction of maximum charge transfer, and thus closely aligned with the c crystallographic axis. Additional vibrational structure is due to TCNQ modes of other symmetry[13] as well as those of the N-dimethyl morpholinium donor cation.

b. Perpendicular to R_{max}. The reflectivity perpendicular to the maximum reflectance on the (010) face is low ($\approx 10\%$), flat, and almost featureless (Fig. 4). No temperature dependence was observed in the infrared. At higher energies, there is a small absorption at $\approx 10\,000$ cm^{-1}, and a strong feature centered at $\approx 18\,000$ cm^{-1}. The absorption at $\approx 18\,000$ cm^{-1} is probably attributable to a localized excitation of the TCNQ molecule.[12,26]

The extreme anisotropy observed between the two polarizations in $DMTM(TCNQ)_2$ on this face of the crystal has been observed for many other TCNQ charge-transfer salts as well,[11–14] once again clearly emphasizing the spectroscopic uniqueness of the TCNQ stacking direction. Additionally, absence of charge transfer and electron-phonon coupling features in the perpendicular polarization provides proof that the polarizers were correctly positioned.[11,12]

Although the direction perpendicular to R_{max} on the (010) face is most likely a principal axis of the crystal, this particular polarization is relatively uninteresting. It lacks temperature dependence and electron-phonon coupling in the infrared and provides no information on the structural phase transition. Consequently, for the majority of this paper, we will confine our discussions to the data in the R_{max} direction on the (010) crystal face.

2. Temperature dependence

To compare the spectral differences between the high- and low-temperature phases in the R_{max} direction on the (010) crystal face, the reflectivity and the frequency-dependent conductivity are shown in Fig. 5 for two temperatures, 300 and 150 K.

Important changes in the electronic state occur as a result of the phase transition in the R_{max} direction. Figure 6 illustrates the strong temperature dependence of the mid-infrared excitation centered at 3200 cm^{-1}. The oscillator strength of this band increases systematically with decreasing temperature within each phase—a trend which is especially pronounced in the low-temperature phase. As shown in Fig. 5, the position of the sharp plasma edge and deep minimum in the reflectivity is redshifted in the low-temperature phase.

A second charge-transfer band occurs at $\approx 10\,500$ cm^{-1} for both 300 and 150 K (Fig. 5). The general shape and oscillator strength of this band is strongly affected by the structural phase transition. In the high-temperature phase, the oscillator strength of this absorption is relatively small, but below T_c, this high-energy excitation appears as a strong doublet. The difference between the two phases is striking, and is an effect not seen in other quarter-filled TCNQ salts.

The infrared reflectance spectra exhibit few changes around T_c (272 K) as a function of temperature. The overall character of the electron-phonon coupling is relatively unaffected by the phase transition. In the low-temperature phase, the A_g phonon modes do not show the pronounced fine structure that was observed in $NPrQn(TCNQ)_2$ and others, which would be indicative of a separation of charge.[29,30] However, careful examina-

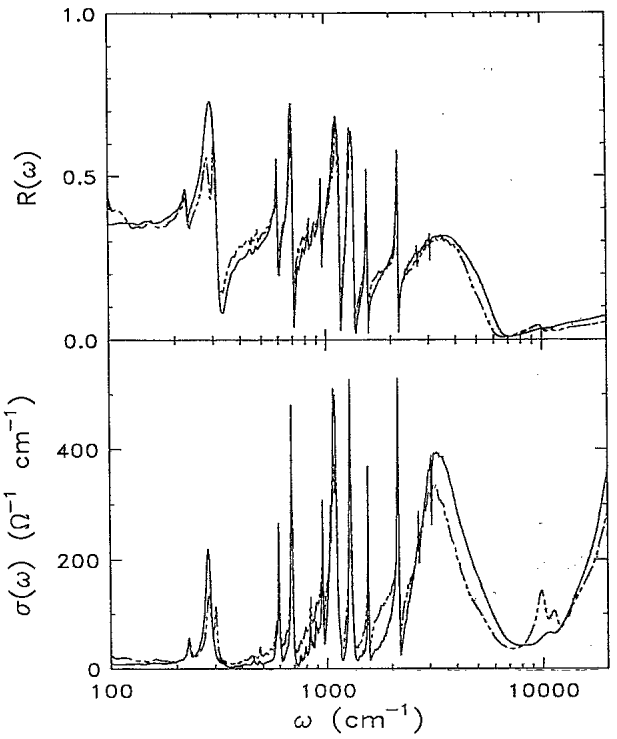

FIG. 5. Reflectance (upper panel) and frequency-dependent conductivity (lower panel) of $DMTM(TCNQ)_2$, with light polarized along the maximum reflectance direction on the (010) crystal face at 300 K (solid line) and 150 K (dashed line).

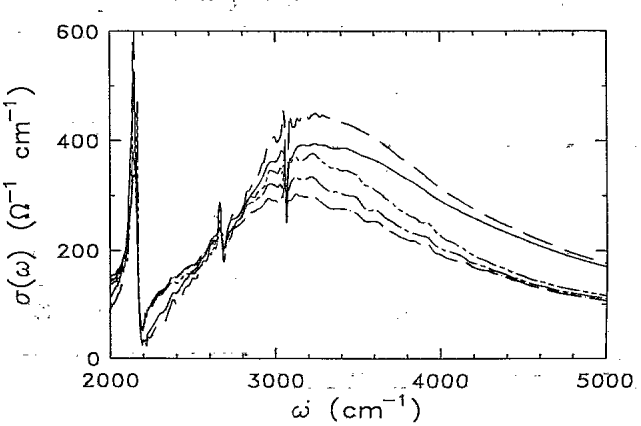

FIG. 6. Detailed temperature dependence of the mid-infrared charge-transfer band in the R_{max} direction on the (010) crystal face. Solid line, 300 K; dashed line, 285 K; dashed-dotted line, 250 K; single-dashed line, 150 K; double-dashed line, 60 K.

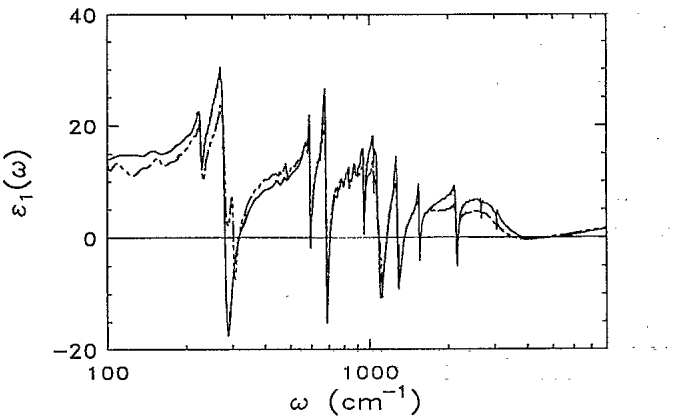

FIG. 7. Real part of the dielectric function, obtained by Kramers-Kronig analysis of the power reflectance of $DMTM(TCNQ)_2$, with light polarized along the maximum reflectance direction on the (010) crystal face at 300 K (solid line) and 150 K (dashed line).

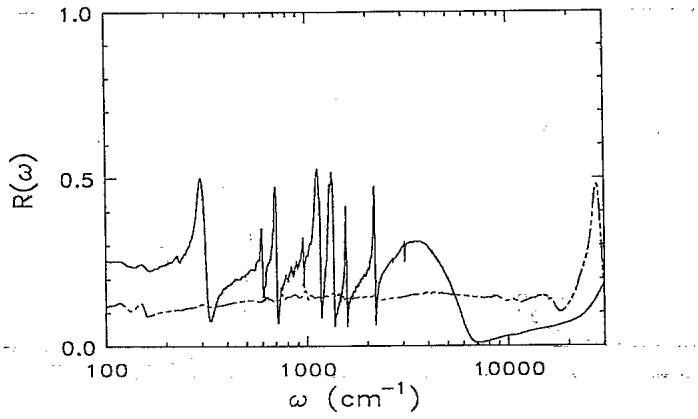

FIG. 8. Room-temperatue reflectance of $DMTM(TCNQ)_2$, with light polarized along the maximum reflectivity (the c crystallographic axis) and perpendicular to the maximum on the (110) crystal face.

tion of the A_g phonon modes in the low-temperature phase reveals very slight multiplet splitting at the crest of some of these modes. Such splitting is probably a result of the reduced molecular site symmetry below the phase-transition temperature.

Extrapolating the frequency-dependent conductivity to zero frequency, we obtain an estimate of the dc conductivity of $\approx 1\ \Omega^{-1}\,\mathrm{cm}^{-1}$ at 300 K. This value is in reasonable agreement with that obtained by four-probe measurements.[1,2]

The real part of the dielectric function, $\epsilon_1(\omega)$, is presented in Fig. 7. Many of the infrared conductivity maxima are intense enough to give a negative dielectric function between transverse (ω_{TO}) and optical (ω_{LO}), frequencies. The mid-infrared charge-transfer excitation drives $\epsilon_1(\omega)$ slightly negative in both phases, although it is more pronounced below T_c. In addition, the screened plasma frequency is redshifted in the low-temperature phase. Extrapolating the low-frequency far-infrared data to zero frequency, we estimate the static dielectric constant of the two phases to be $\epsilon(0)\simeq 17$ at 300 K and $\epsilon(0)\simeq 19$ at 150 K. We are presently unaware of any microwave measurements of the static dielectric constant in $DMTM(TCNQ)_2$, so comparison with our extrapolated data is not possible. We estimate the high-frequency (above 8000 cm^{-1}) dielectric constant, ϵ_∞, to be 1.5 and 1.7 in the high- and low-temperature phases, respectively.

B. (110) crystal face

1. R_{max} direction

On the (110) face of the single-crystal samples, R_{max} is polarized purely along the c crystallographic axis. Consequently, the ir and visible spectra are very similar (in terms of the electron-phonon coupling and infrared excitations) to that in the R_{max} on the (010) crystal face. The temperature dependence is also analogous to what we obtained on the other face. However, from examination of Fig. 8, it is evident that the phonon lines along c on this face are not as intense or as well shaped as those measured along the R_{max} direction on the (010) face, suggesting that the direction of maximum charge transport is not directly along the c axis. From the ratio of phonon peak heights, we estimate that the angle between R_{max} on the (010) crystal face and R_{max} (the c crystallographic axis) on the (110) side is $\approx 20°$. This is in good agreement with that expected from the crystal structure.[3–5] Consequently, we conclude that the TCNQ stacking direction c is not a principal axis of the dielectric tensor. Thus, for the remainder of the paper and especially in our discussion of the electron-phonon coupling effects, we concentrate on the spectra along R_{max} on the (010) crystal face, which we believe is a principal axis of the crystal.

2. Perpendicular to R_{max}

Perpendicular to the R_{max} direction on the (110) face of the crystal, we measure a combination of two principal axis reflectivities, shown in Fig. 8. The major component of this polarization is b, the axis directed along the length of the TCNQ molecule. As in the spectra taken of the (010) crystal face, there is extreme anisotropy between the two polarizations. The complete absence of electron-phonon coupling and the low-energy charge-transfer excitation in the direction perpendicular to c can again be taken as proof of the correctness of the polarizer positions.

In the infrared, the reflectivity is low and flat, with a few weak phonons and no temperature dependence. In the low-temperature phase, we found no evidence of a low-energy excitation at 430 cm^{-1}, attributable to a reduced band gap, as expected from the crystal-field distortion theory of the phase transition. The frequency-dependent conductivity, shown in Fig. 9, is close to zero below about 4000 cm^{-1}. $\sigma_1(\omega)$ is actually slightly negative in the far-infrared, probably due to small errors in measuring the reflectivity. We consider $\sigma(\omega)$ to be effectively zero in this regime. The frequency-dependent conductivity begins to rise at $\approx$4000 cm^{-1} in both phases. In the near-infrared and visible frequency range,

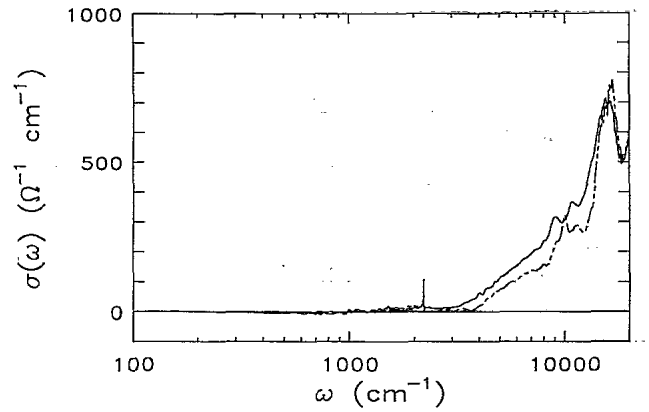

FIG. 9. Frequency-dependent conductivity of $DMTM(TCNQ)_2$ with light polarized perpendicular to the c crystallographic axis on the (110) face at 300 K (solid line) and 150 K (dashed line). The conductivity is essentially zero below 4000 cm^{-1} (0.5 eV).

there is strong temperature dependence, especially around 10 000 cm^{-1}. Among the more interesting electronic features is the strong absorption at ≈ 2 eV in both phases, which is often associated with intramolecular excitations within a doubly charged dimer.[31] Finally, the strong excitation centered at $\approx 23\,000$ cm^{-1} seen in the reflectance spectrum of Fig. 8 may be due to a localized excitation polarized along the long axis of the TCNQ molecule.[25,26]

IV. DISCUSSION

A. (010) crystal face

1. *Electronic features along* R_{max}

Above T_c, the spectra of $DMTM(TCNQ)_2$ along the R_{max} direction on the large (010) crystal face shows qualitative agreement with other "quarter-filled," 1:2 semiconducting charge-transfer materials in terms of the position and intensity of the electronic and vibrational features.[11–15] The similarity between our data at 300 K and those of Rice, Yartsev, and Jacobsen[15] for the $MEM(TCNQ)_2$ system at room temperature (the dimerized phase) is particularly striking.

For strongly dimerized, large U materials, the high-energy spectral features polarized closely along TCNQ stacking direction typically consist of two strong, broad absorptions which correspond to electronic charge transfer between TCNQ moieties within the chain.[25,26] The absorption band centered in the mid-infrared corresponds to the charge transfer: $TCNQ^0+TCNQ^- \rightarrow TCNQ^-+TCNQ^0$.[13,26] Despite differences in the chemical natures of the donor cation in $MEM(TCNQ)_2$ and $DMTM(TCNQ)_2$, the low-energy electronic excitations of the TCNQ chain are nearly identical, centered at ≈ 3200 cm^{-1}

In $DMTM(TCNQ)_2$, the center frequency and integrated oscillator strength of the mid-infrared band is a strong function of temperature, increasing systematically with decreasing temperature within each phase. This trend is especially pronounced in the low-temperature phase, and correlates inversely with the dc conductivity. For example, at 250 K, σ_{dc} is a maximum, but the oscillator strength of the mid-infrared band is a minimum. However, we find no evidence that this "missing oscillator strength" at 250 K has shifted to lower frequency, as might be expected for increased conductivity. (See the later discussion of the sum rule.) At the present time, we have no explanation for this phenomenon.

The temperature dependence of these electronic features have important implications for charge transport in the TCNQ stacking direction. Yartsev and Graja[6,7] have proposed that electron hopping between molecular clusters may be responsible for the activated nature of the dc conductivity in dimerized salts. Based upon this model and the average value of the static charge transfer,[32] we calculate $E_A = 0.30$ eV in the high-temperature phase, in reasonable agreement with that reported from transport measurements.[1,2] Consequently, we may conclude that the mechanism of charge transport above T_c is dominated by hopping between isolated dimers. However, in the low-temperature phase, we find poor agreement between the activation energy transport as calculated by this method and the experimental value of 0.03 eV. Thus, we must conclude that charge transport is not dominated by hopping along the TCNQ chain below T_c; it must occur by an entirely different mechanism.

As shown in Fig. 5, the position of the deep plasma minimum in the reflectivity is redshifted in the low-temperature phase. Redshifts of these features are rather unusual.[11,14] The classical plasma frequency is defined as

$$\tilde{\omega}_p^2 = \frac{4\pi n e^2}{\epsilon_\infty m^*} ; \qquad (2)$$

thus, the observed spectral modifications may result from (i) a decrease in the band curvature (increase in m^*), (ii) a reduction in the number of conduction electrons at T_c, or (iii) an increase in ϵ_∞ due to the increased strength of the U band. From the partial sum rule, we estimate the effective band mass to be $m^* = 1.5m_e$ and $m^* = 1.8m_e$ in the high- and low-temperature phases, respectively, supporting the band curvature proposal. For additional details, refer to the later discussion of the sum rule.

A second higher-energy charge-transfer band is observed in our spectra at $\approx 10\,500$ cm^{-1} and can be attributed to the charge-transfer process: $TCNQ^- + TCNQ^- \rightarrow TCNQ^0 + TCNQ^{=}$.[13,26] Because two electrons reside on the same site in the final state, the energy of this transition is proportional to an effective Hubbard U, the on-site Coulomb repulsion.[33] From the center position of this band, we obtain an estimate for the effective on-site Hubbard parameter of 10 500 cm^{-1} (1.30 eV) for both phases of $DMTM(TCNQ)_2$, which is comparable to values obtained for other TCNQ charge-transfer salts.[12,13]

In $DMTM(TCNQ)_2$, the shape and oscillator strength of the higher-energy excitation display strong tempera-

ture dependence. The excitation at 10 500 cm^{-1} is weak in the high-temperature phase. However, in the low-temperature phase, this band appears as a strong doublet. The fundamental nature of such a doublet structure is not well understood.[11–14]

The weak absorption of the U band in the high-temperature phase suggests that few electrons occupy adjacent sites along the chain, possibly resulting in a low dc conductivity. In contrast, the increased oscillator strength of the U band below T_c suggests that the charged electrons are occupying adjacent sites more frequently. That the electrons are much closer together in the low-temperature phase without a significant change in the magnitude of the on-site Coulomb repulsion suggests that the effect of the long-range Coulomb interaction may be decreased. Such a charge reorganization may be responsible for the increased conductivity.

2. *Phonon features along* R_{max}

Among the most prominent and interesting spectral features of TCNQ charge-transfer salts are the ten in-plane A_g vibrational modes of the TCNQ molecule, activated by coupling to the charge-transfer excitations.[13–15,17,27,28] All ten A_g modes are observed in $DMTM(TCNQ)_2$, most with relatively strong intensity. In the high-temperature phase, the vibrational structure is very similar to that in the $MEM(TCNQ)_2$ system. A comparison of the electron-phonon coupling in $DMTM(TCNQ)_2$ with that in the MEM system will be discussed in some detail in the following two sections.

The overall character of the electron-phonon coupling in $DMTM(TCNQ)_2$ is relatively unaffected by the structural phase transition at 272 K. Below T_c, the A_g phonon modes in $DMTM(TCNQ)_2$ exhibit no pronounced fine structure, as might be expected in light of the evidence of several independent investigations[1,2,10] which imply two inequivalent TCNQ chains per unit cell—one with and one without a $2k_F$ distortion. The only spectral evidence to support this hypothesis is the very slight multiplet splitting at the crest of some of the A_g modes. This splitting is probably a result of the reduced symmetry below the phase-transition temperature, and therefore related to the inequivalence of the TCNQ stacks.

a. Dimer model. The infrared spectra of typical insulating 1:2 compounds are dominated by electron localization effects,[11–14] suggesting that the TCNQ stack may be well described by linear cluster models of dimers, trimers, or tetramers.

The solution of the coupled electron-phonon problem for an isolated TCNQ dimer with one electron per two TCNQ molecules has been given by Rice, Yartsev, and Jacobsen.[15] The complex dielectric function is

$$\tilde{\epsilon}(\omega)=\epsilon_\infty+\frac{4\pi n e^2 d^2(2t^2/\omega_{CT})}{\omega_{CT}^2[1-D(\omega)]-\omega^2-i\omega\Gamma}, \quad (3)$$

where ω_{CT} determines the position of the charge-transfer peak in the absence of vibrational coupling, Γ is an electronic relaxation rate, and ϵ_∞ is the background dielectric constant. Here, t is the chain-axis transfer integral, d is the spacing between the molecules, and $n=N/V$ is the molecular density (N is the number of molecules in the cluster and V is the volume of the system). The function

$$D(\omega)=\sum_\alpha \frac{\lambda_\alpha \omega_\alpha^2}{\omega_\alpha^2-\omega^2-i\omega\gamma_\alpha} \quad (4)$$

is the phonon propagator. The ω_α and γ_α refer to the unperturbed resonant frequencies if the totally symmetric vibrational modes and corresponding linewidths, respectively. The λ_α are dimensionless coupling constants, related to the electron-molecular-vibration (EMV) coupling constants (g_α's) by

$$\lambda_\alpha=\frac{8t^2 g_\alpha^2}{\omega_{CT}^3 \omega_\alpha}. \quad (5)$$

Based upon structural evidence[4,5] and the similarity of our spectra with that of $MEM(TCNQ)_2$, we have analyzed our infrared results within the framework of this isolated dimer model.[15] The dimer model has been fitted to the experimental optical conductivity at room temperature using a nonlinear least-squares method; the results are shown in Fig. 10. The structural parameters used in the calculation were the separation between the TCNQ molecules $d=3.25$ Å and the unit-cell volume $V=1385$ $Å^3$. The fitted parameters for the charge-transfer band are a transfer integral of $t=1957$ cm^{-1}, in good agreement with that expected from the sum rule. The charge-transfer energy and electronic linewidth are $\omega_{CT}=3165$ cm^{-1} and $\Gamma=2203$ cm^{-1}. The experimental values for the unperturbed phonon frequencies, linewidths, and the EMV coupling constants for $DMTM(TCNQ)_2$ at room temperature are shown in Table I, along with the calculated A_g modes of the $TCNQ^-$ molecule by Bozio, Girlando, and Pecile[34] and the values for the EMV coupling

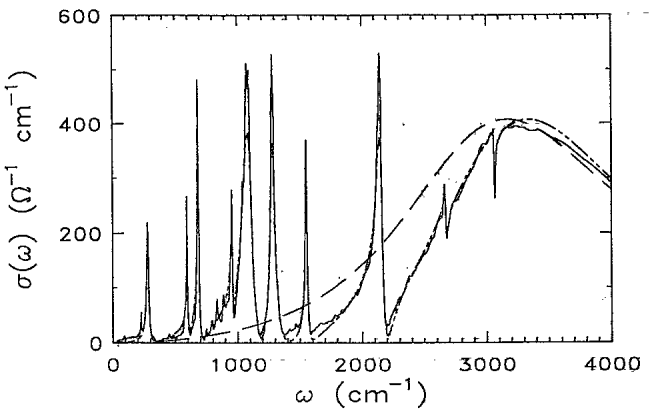

FIG. 10. The fit using the dimer model of Rice *et al.* to the frequency-dependent conductivity of $DMTM(TCNQ)_2$ at 300 K for R_{max} on the large (010) crystal face. The solid line is the experimental data, the double-dashed line is the best fit to the data with the charge-transfer parameters $t=1957$ cm^{-1}, $\omega_{CT}=3165$ cm^{-1}, and $\Gamma=2203$ cm^{-1} (other parameters are listed in Table I), and the dashed line is the electronic continuum in the absence of any electron-phonon coupling. Note that the phonon intensities are not well reproduced.

constants based on *a priori* calculations by Lipari *et al.*,[35] as well as the dimer model results for $MEM(TCNQ)_2$ at 300 K by Rice, Yartsev, and Jacobsen.[15] Neither the frequencies nor the coupling constants of $DMTM(TCNQ)_2$ were observed to be a function of temperature within experimental error. Temperature dependence of the frequencies of the EMV coupling constants is not observed in the $MEM(TCNQ)_2$ system either.[15,18]

The fitted values of the unperturbed phonon frequencies of $DMTM(TCNQ)_2$ (Table I) are in good agreement with those determined for $MEM(TCNQ)_2$ and also with the calculated frequencies for a $TCNQ^-$ molecule. The coincidence is slightly better for the lower-energy modes, a trend which we do not understand at the present time. The EMV coupling constants agree well with tabulated values for other TCNQ salts, calculated using the dimer model.[36] However, the dimer-model calculations for the EMV coupling constants are smaller than those predicted by the *a priori* calculations, an effect which has also been observed in some of the TMTSF charge-transfer salts.[37] A plot of $\mathrm{Re}(1/\sigma_1(\omega))$ gives similar frequencies and coupling constants.[19]

While the dimer-model fit in Fig. 10 approximates the experimental data fairly well, it fails in a number of important aspects. One of the difficulties in fitting the dimer model to the optical conductivity stems from the fact that the phonon conductivities can never exceed that of the central charge-transfer band, regardless of how large the EMV coupling constant becomes. Thus, the intensity of some of the A_g modes cannot be reproduced. Furthermore, the transfer integral and the position of the charge-transfer band cannot be determined self-consistently. The spectrum of excitations in a dimer requires that $\omega_{CT} \geq 2t$. However, $t = 1957\ \mathrm{cm}^{-1}$, which requires that $\omega_{CT} \geq 3900\ \mathrm{cm}^{-1}$, higher than observed. This implies that a significant portion of the conductivity may arise from interband transitions rather than from charge-transfer excitations. This result is not too surprising given the fact that this system is only weakly dimerized and not as localized (based on the larger value of the 300 K dc conductivity) as $MEM(TCNQ)_2$. The two-dimensional nature of the sulfur atom in the DMTM cation may also play a role in the increased dimensionality.

b. Phase phonon model. An alternative model of

TABLE I. The calculated A_g mode frequencies and linear electron-molecular-vibrational coupling constants, and the vibronic parameters used in the dimer model fit to $DMTM(TCNQ)_2$.

	Calculated $(TCNQ^-)$[a]		$DMTM(TCNQ)_2$[b]			$MEM(TCNQ)_2$[c]	
A_g mode	ω_α (cm^{-1})	g_α (cm^{-1})	ω_α (cm^{-1})	γ_α (cm^{-1})	g_α (cm^{-1})	ω_α (cm^{-1})	g_α (cm^{-1})
ν_1	3052	31	3065	8	51	3070	40
$2\nu_4$?	2806		2676	12	58		
ν_2	2193	423	2200	6	302	2210	403
ν_3	1603	1057	1593	6	359	1630	468
ν_4	1403	392	1406	6	485	1395	363
ν_5	1209	229	1186	6	272	1180	298
ν_6	968	237	963	4	69	958	89
ν_7	731	263	716	6	192	718	210
ν_8	607	18	603	4	88	597	97
ν_9	336	194	324	8	210	324	177
ν_{10}	148	78				150	73

[a] R. Bozio, A. Girlando and C. Pecile, J. Chem. Soc. Faraday Trans. II, 71, 1237 (1975); N.O. Lipari, M.J. Rice, C.B. Duke, R. Bozio, A. Girlando, and C. Pecile, Int. J. Quant. Chem. 11, 583 (1977) (*a priori* calculations for TTF-TCNQ).

[b] Parameters used are $t = 1957\ \mathrm{cm}^{-1}$, $\omega_{CT} = 3165\ \mathrm{cm}^{-1}$, and $\Gamma = 2203\ \mathrm{cm}^{-1}$.

[c] M.J. Rice, V.M. Yartsev, and C.S. Jacobsen, Phys. Rev. B 21, 3437 (1980).

electron-phonon coupling which we have applied to the optical conductivity of $DMTM(TCNQ)_2$ at 300 and 150 K is that of Bozio, Meneghetti, and Pecile[17] for one-dimensional systems with twofold-commensurate charge-density waves (CDW). This model is an extension of earlier work on commensurate one-dimensional CDW systems[38] and phase-phonon models.[16] The optical conductivity is calculated from the complex dielectric function

$$\tilde{\epsilon}(\omega)=\epsilon_\infty-\frac{4\pi}{NV_m}\left[\chi(\omega)+\sum_\alpha I_\alpha(\omega)\langle Q_\alpha(\omega)\rangle/E(\omega)\right], \tag{6}$$

where V_m is the volume per TCNQ molecule and N is the number of molecules in the chain. The important terms in Eq. (6) are $\chi(\omega)$, I_α, $\langle Q_\alpha(\omega)\rangle$, and $E(\omega)$. These are defined in the following way. First,

$$\chi(\omega)=\sum_k\sum_{n,m}\frac{\hbar^2}{(E_{kn}-E_{km})}\frac{n(E_{kn})-n(E_{km})}{E_{kn}-E_{km}-\hbar\omega-i\hbar\Gamma}\times|j_{nm}(k,0)|^2 \tag{7}$$

is the dielectric susceptibility for a single-particle excitation across the gap. Here $E_{kn}=(-1)^{n+1}\sqrt{\epsilon_k^2+|\Delta_k|^2}$ are the energy bands, with $\epsilon_k=-2t\cos(kd)$ and $\Delta_k=\Delta_s+i\Delta_b\sin(kd)$ indicating the nature of the distortion gap [s for site-centered or b for bond-centered charge-density waves (CDW's)]. $\Delta_s\neq0$ is associated with an alternating molecular distortion (AMD). However, no AMD is observed in $DMTM(TCNQ)_2$, so it is assumed that $\Delta_s=0$. $n(E_{kn})$ is the Fermi-Dirac distribution function for spinless fermions,[39] and $j_{nm}(k,0)$ are the matrix elements of the current operator for a distorted linear chain.[17,40] The quantity $\langle Q_\alpha(\omega)\rangle$ is a Fourier transformed generalized coordinate and is defined by the relation

$$\langle Q_\alpha(\omega)\rangle=D_\alpha^{i,e}(\omega)\left[\sum_{\beta=1}^{n}T_{\alpha\beta}(\omega)\langle Q_\beta(\omega)\rangle+E(\omega)I_\alpha(\omega)\right]. \tag{8}$$

Here,

$$D_\alpha^i(\omega)=\frac{2\omega_\alpha}{\hbar[(\omega+i\gamma_\alpha)^2-\omega_\alpha^2]} \tag{9}$$

is the phonon propagator for the A_g internal modes, each of which is characterized by an unperturbed frequency ω_α, a linewidth γ_α, and an EMV linear coupling constant g_α. Finally, $T_{\alpha\beta}(\omega)$ and $I_\alpha(\omega)$ may be described in phenomenological terms as a phonon-phonon (self) interaction, and a phonon-amplitude function. For details, refer to Ref. 17. The indices α and β refer to the internal modes. Finally, $E(\omega)$ is the incident electric field.

We calculate the contribution of the cation counterchains to the total distortion gap as

$$\Delta_b=B_x+\left[\frac{\partial t}{\partial u}\right]_0 u_0, \tag{10}$$

where B_x is the counterion contribution and $(\partial t/\partial u)_0$ is the linear coupling of the electrons to the acoustic mode.[17]

The frequency shifts of the phonons from the unperturbed values were calculated to first order using[17]

$$\delta_\alpha=\frac{g_\alpha^2}{2\pi t}K(1-\Delta_b^2/4t^2), \tag{11}$$

where $K(x)$ is a complete elliptic integral of the first kind.

Because Eq. (8) consists of n coupled inhomogenous linear equations, analytic solutions for $\langle Q_\alpha(\omega)\rangle$ are tedious for large systems and numerical methods are required. The techniques used here to solve for $\langle Q_\alpha(\omega)\rangle$ have been previously described,[41] and extended to allow the model to be fit to the data using a least-squares method. Using this model, what we calculate are the optical properties due to interband transitions and phase phonon modes in the $U\rightarrow\infty$ limit for a *half-filled* system of spinless electrons (or holes). This is the appropriate case for $DMTM(TCNQ)_2$, a *quarter-filled* system, which, in the limit of large U, has a half-filled lower Hubbard band.

Initial fits agreed well with the data at low frequencies, but gave values too large for the conductivity at high frequencies. This larger oscillator strength can be attributed to the neglect of the upper Hubbard band in the model. To solve this problem a phenomenological approach was taken where the energy bands were rescaled by introducing an effective transfer integral $t'=\xi t$. The other parameters in the calculation must also be rescaled $g'_\alpha=\sqrt{\xi}g_\alpha$ and $\tilde{\epsilon}'(\omega)=\xi\tilde{\epsilon}(\omega)$, where ξ is the scaling parameter.[42] As Fig. 11 shows, at high frequency the result for $\xi=2$ is much better than that for $\xi=1$; this suggests that rescaling the energy bands may be a good approximation of the band structure of quarter-filled systems. Only the results

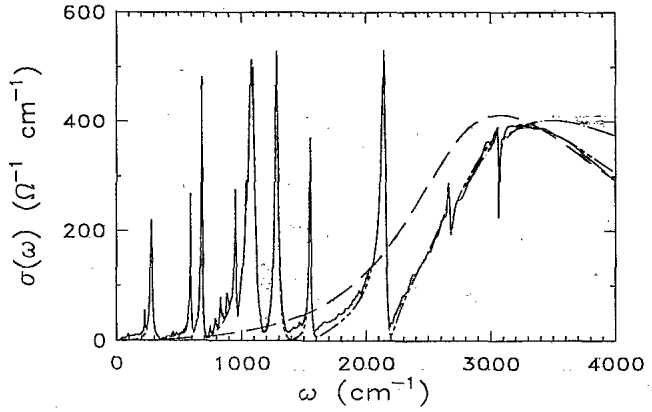

FIG. 11. The fit using the phase phonon model of Bozio *et al.* to the frequency-dependent conductivity of $DMTM(TCNQ)_2$ at 300 K for R_{max} on the large (010) crystal face. The solid line is the experimental data; the single-dash line is the fit to the data for $\xi=1$ and the double-dashed line is for $\xi=2$. The dashed line is the bare electronic continuum for $\xi=2$. The electronic parameters used in the model ($\xi=2$) are $t=1853$ cm^{-1}, $2\Delta=2685$ cm^{-1}, and $\Gamma=763$ cm^{-1}. Other parameters are listed in Table II. Note that the phonon intensities are reproduced quite well.

for $\xi=2$ will be presented here (although only t and Γ are observed to change noticeably with ξ).

The results of the model fit to the frequency-dependent conductivity at room temperature and 150 K are shown in Figs. 11 and 12 respectively; the parameters used are listed in Table II. Overall, the line shapes and intensities of the phonons (the A_g vibrations of the TCNQ molecule) are all reproduced extremely well (a clear improvement on the dimer model), and the calculated EMV coupling constants are in good agreement with *a priori* calculations and phase-phonon model estimates for TCNQ salts of this type.[43,35]

At 300 K, a good quality fit was obtained using $t=1853$ cm^{-1}, $\Delta=2685$ cm^{-1}, and $\Gamma=763$ cm^{-1}. We find that the contribution of the static cation counterchain potential to $2\Delta_b$ is 98%, indicating that the nature of the distortion is mediated by the cation counterchains rather than an intrinsic stack distortion (a result that is not uncommon for weakly dimerized systems[17,41]).

The result of the fit to the 150-K data indicates that the electronic behavior of the system has become much more complicated. While t and 2Δ have decreased to

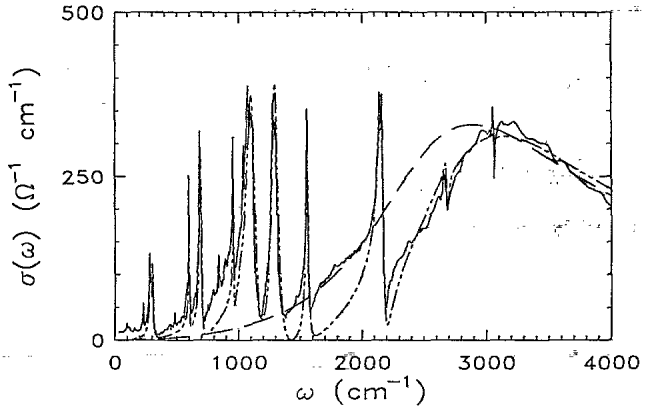

FIG. 12. The fit using the phase phonon model by Bozio *et al.* to the frequency-dependent conductivity of DMTM(TCNQ)$_2$ at 150 K for R_{max} on the large (010) crystal face. The solid line is the experimental data and the double-dashed line is the fit to the data for $\xi=2$. The dashed line is the bare electronic continuum for $\xi=2$. The electronic parameters used in the model ($\xi=2$) are $t=1476$ cm^{-1}, $2\Delta=2455$ cm^{-1}, and $\Gamma=811$ cm^{-1}. Other parameters used are listed in Table II. Note the heavy residual conductivity below 2Δ.

TABLE II. One-dimensional twofold-commesurate CDW model parameters for a *b*-CDW for the fit to the optical conductivity of DMTM(TCNQ)$_2$ for radiation polarized parallel to the chain direction at room temperature and 150 K.[a]

T	300 K				150 K			
t	1853 cm^{-1}				1476 cm^{-1}			
2Δ	2685 cm^{-1}				2455 cm^{-1}			
Γ	763 cm^{-1}				811 cm^{-1}			
V_m	692 Å^3				685 Å^3			
A_g mode	ω_α (cm^{-1})	(δ_α) (cm^{-1})	γ_α (cm^{-1})	g_α (cm^{-1})	ω_α (cm^{-1})	(δ_α) (cm^{-1})	γ_α (cm^{-1})	g_α (cm^{-1})
ν_1	3064	(1)	3	81	3066	(1)	2	52
$2\nu_4$?	2675	(1)	6	94	2686	(2)	6	87
ν_2	2200	(41)	2	532	2202	(37)	5	434
ν_3	1595	(60)	4	645	1618	(95)	5	691
ν_4	1410	(104)	2	847	1435	(97)	1	700
ν_5	1188	(32)	6	470	1187	(27)	10	372
ν_6	962	(2)	4	124	960	(2)	3	88
ν_7	717	(17)	1	342	725	(18)	4	303
ν_8	603	(4)	2	154	606	(3)	3	130
ν_9	329	(22)	6	386	330	(16)	5	286
					292	(1)	7	81

[a] In the calculations $d=3.25$ Å, $u_0=0.02$ Å, and N=256.

1476 and 2455 cm^{-1}, respectively, the interband damping has *increased* to 811 cm^{-1}. The vibronic parameters do not change appreciably (see Table II). However, the phonon line shapes are not well reproduced in the neighborhood of 2Δ, and in general there is a lot of residual conductivity below the gap. The contribution of the cation potential to $2\Delta_b$ decreases to 95% below T_c. This change in the influence of the static potential may be related to the possible ordering of the DMTM cations below T_c. Regardless of whether the DMTM cations order or not, the TCNQ stacks are inequivalent below T_c; thus, if there are slightly different distortion potentials on the stacks, then that might be responsible for the peculiar shape of the conductivity near 2Δ.

In both the high- and low-temperature phases, the model value for the semiconducting energy gap is $2\Delta \approx 2500$ cm^{-1} (0.3 eV). While this value is in good agreement with the infrared threshold (≈ 2100 cm^{-1}) in the high- and low-temperature phases (Figs. 5 and 6), it contrasts significantly with transport measurement estimates of 2Δ both above (0.52 eV) and below (0.06 eV) T_c.

3. *Additional vibrational features*

Finally, we would like to discuss a few additional vibrational features which remain unaccounted for within the isolated dimer and the twofold-commensurate CDW models (refer to Fig. 4). We observe several modes of non-A_g symmetry for the TCNQ molecule which are in good agreement with expected resonance positions.[13] As expected, they are much less intense than the A_g modes. We also observe an interesting antiresonance at 2675 cm^{-1}. Although it is not among the 54 normal modes of the TCNQ molecule, it has also been observed[44,15] in $TEA(TCNQ)_2$ and $MEM(TCNQ)_2$. We believe that this unusual feature is an overtone of the $\nu_4(A_g)$ mode in the TCNQ molecule which occurs at 1403 cm^{-1}, as it is slightly less (≈ 100 cm^{-1}) than twice the frequency of the 1403-cm^{-1} mode.

4. *Sum rule*

Information about the effective number of electrons involved in optical transitions can be obtained from the partial sum rule[24]

$$\left[\frac{m}{m^*}\right] N_{\text{eff}}(\omega) = \frac{m}{32\pi N_c e^2} \int_0^{\omega} \sigma_1(\omega')\, d\omega' \ , \qquad (12)$$

where m^* is the effective mass of the carriers and N_c is the number of condition electrons per unit volume. A plot of this function is shown in Fig. 13 for the electric-field vector polarized along $R_{\max}$ (close to the chain direction on the large crystal face) at 300 and 150 K, as well as perpendicular to the $R_{\max}$ direction on the same face at 300 K.

In the direction close to the dimer axis, $(m/m^*)N_{\text{eff}}$ rises rapidly in the low-frequency region, leveling off above 5000 cm^{-1}. From the plateau values of the integrated oscillator strength in the near-infrared, we estimate $m^* = 1.5 m_e$ and $m^* = 1.8 m_e$ in the high- and low-temperature phases, respectively, assuming $N_{\text{eff}} = 0.5$. The integrated oscillator strength of the vibrational features does not vary significantly with temperature. At higher energy, the increased oscillator strength due to the mid-infrared charge-transfer band is readily evident. In $DMTM(TCNQ)_2$, the integrated oscillator strength of this band is a strong function of temperature, increasing systematically with decreasing temperature within each phase (Fig. 6). However, as illustrated in Fig. 13, we find no evidence that this "missing oscillator strength" at 250 K has shifted to lower frequency, as might be expected for increased conductivity. In fact, it has shifted to higher energies. The enhanced contribution of the 10 500-cm^{-1} charge-transfer band is seen in the $T = 150$ K data. The two curves come together nicely at higher frequency, demonstrating conservation of oscillator strength above and below T_c. In the direction perpendicular to the chain axis, $(m/m^*)N_{\text{eff}}$ is small in the infrared but rises rapidly at higher frequencies.

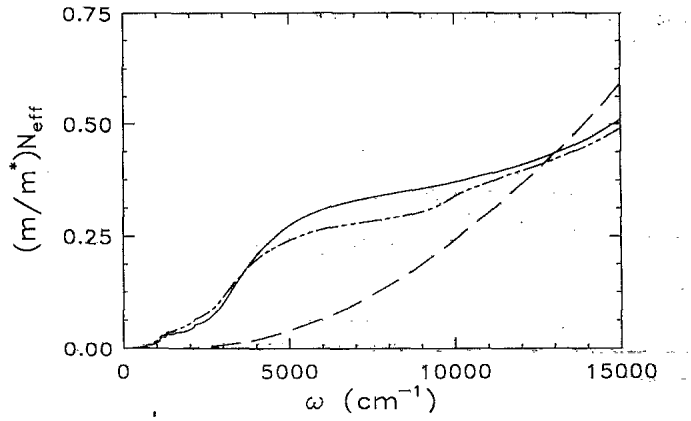

FIG. 13. Sum rule for $DMTM(TCNQ)_2$ for the maximum reflectance direction on the (010) crystal face at 300 and 150 K and for the perpendicular polarization on the same crystal face at 300 K.

B. (110) crystal face

On the (110) face of the crystal, the maximum reflectance is along the c crystal logographic axis. As the behavior of these spectra is so similar to that along $R_{\max}$ on the (010) face, the following discussion will be confined to the spectra taken in the direction perpendicular to $R_{\max}$ on the short (110) side. The major component in this direction is the b crystallographic axis, which is along the long axis of the TCNQ molecule and a principal axis of the crystal.

1. *Proposed structural distortion along the b axis*

It has been postulated that the dramatic increase in the dc conductivity in $DMTM(TCNQ)_2$ is a result of a crystal-field distortion at T_c.[3] Figure 2 shows the band structure in the high- and low-temperature phases of the salt as proposed by Visser *et al.*[3] An identical set of bands is located at higher energy, separated from those shown in Fig. 2 by the Hubbard gap. Spectral transitions

occur between the various energy levels.

Based upon the band structure in Fig. 2, we expect the electronic spectrum to be quite simple in the high-temperature phase, having only one main excitation within the manifold at low energy. Because the activation energy for conduction has been measured to be 0.26 eV,[1,2] we can approximate the resultant band gap to be 0.52 eV or 4200 cm^{-1}. We would also expect to see several higher-energy features, including an excitation across the Hubbard gap near ≈ 1.3 eV (or 10 500 cm^{-1}) and a transition to the upper level of the manifold at ≈ 1.82 eV (or 14 700 cm^{-1}), the energy difference between these two features being the 0.52-eV band gap. Transitions originating from excited states will not be observed in the spectra.

In the low-temperature phase, reduction of symmetry splits the bands, and several more transitions become possible. According to the crystal-field distortion theory, four unique transitions should be observed within the manifold at ≈ 430, ≈ 3700, ≈ 4200, and ≈ 7900 cm^{-1}. We are primarily interested in the lowest-energy charge-transfer processes, as they are expected to dominate the conduction process. At higher energy, we expect to observe excitations across the Hubbard gap to various levels in the upper manifold. The three lowest-energy features would be at $\approx 10\,500$, $\approx 14\,200$, and $\approx 14\,600$ cm^{-1}, the energy difference between the last two being essentially the 0.06-eV low-temperature valence- to conduction-band gap.

2. *Comparison with spectra*

Figure 9 shows the experimental frequency-dependent conductivity perpendicular to R_{max} on the (110) crystal face in the high- and low-temperature phases. It remains for us to assess our spectral data in this polarization in terms of the proposed crystal-field distortion along the b axis and the associated band-structure modifications shown in Fig. 2.

As expected, we observe no electronic features in the 300-K spectrum at low energy. However, we also find no evidence of a low-energy charge-transfer band at 430 cm^{-1} in the low-temperature phase of the salt, which would have been expected from the crystal-field splitting. It is anticipated that such an excitation would be strong if interchain charge transfer dominated the conduction process in the low-temperature phase.

In light of the various recent studies[1,2,10] which give great credibility to the crystal-field distortion theory by Visser *et al.*[3], it is not clear why we do not observe conclusive spectral evidence for the low-energy charge transfer at 430 cm^{-1}. One possible explanation is that the physical separation of the TCNQ chains is large due to the DMTM cation sheets, and that the oscillator strength of this transition is small. Another possibility is that some of the lower-energy electronic transitions are either symmetry forbidden or of the wrong symmetry to be observable with electric dipole allowed spectroscopy.[45,46] If the transition were symmetry forbidden, it would not contribute significantly to the conduction process. However, if an excitation does not obey the ir selection rules, it could still contribute to the conduction process. This may explain why low-energy charge transfer is not evident in our spectra below T_c. Low-temperature Raman measurements on DMTM(TCNQ)$_2$ would augment this study nicely.

In both phases, there is an absorption edge at ≈ 4000 cm^{-1}, above which the frequency-dependent conductivity begins to rise rapidly. It is this energy which we attribute to the interchain transport gap, corresponding to an activation energy of ≈ 0.25 eV. This value is in excellent agreement with transport measurements[1,2] and the band-structure predictions of Fig. 2 for the high-temperature phase. However, in the low-temperature phase, according to the band-structure diagram, we should also expect to see evidence for two low-energy charge-transfer bands (at ≈ 430 and ≈ 3800 cm^{-1}). From examination of Fig. 9, it is clear that these are absent.

In the near-infrared and visible frequency range, there is strong temperature dependence in the spectra, especially near 10 000 cm^{-1}. In the high-temperature phase, this feature is a doublet, the splitting between peak centers of the doublet being ≈ 1900 cm^{-1}. Below T_c, the spectra in this region have a triplet structure, the center absorption being most pronounced. Although the main absorption in this frequency region could result from a transition across the Hubbard gap to the lowest-energy band in the second manifold, the doublet and triplet features are not accounted for within the crystal-field splitting theory.

Among the most interesting of the higher-energy features is the strong absorption at ≈ 2 eV. As it is not present in the other two principal axis polarizations which we have discussed, we conclude that it is polarized exclusively in the b crystallographic direction. Although such a strong feature in this frequency regime is often associated with an intramolecular excitation within a doubly charged dimer,[31] we instead believe it is associated with a strongly allowed transition across the Hubbard gap to the upper level of the second manifold. Based upon the crystal-field splitting theory and the associated band-structure modifications (Fig. 2), such a transition is expected to appear at ≈ 1.8 eV. Below T_c a broader band with a slight doublet character might be anticipated due to the reduced symmetry. However, no such temperature dependence is observed in Fig. 9.

V. CONCLUSIONS

We have presented a spectral investigation of DMTM(TCNQ)$_2$ at various temperatures both above and below T_c in an effort to understand the unusual electrical transport properties in the high- and low-temperature phases and gain insight into the mechanism and characteristics of the phase transition. For light polarized close to the TCNQ stacking direction on the (010) face, the ir spectra are characteristic of other quarter-filled, dimerized, 1:2 semiconducting TCNQ charge-transfer salts, with two charge-transfer excitations and prominent A_g vibrational structure. The isolated dimer model of Rice, Yartsev, and Jacobsen[15] and the twofold-commensurate charge-density-wave model by Bozio, Meneghetti, and Pecile[17] were applied to DMTM(TCNQ)$_2$ both above and

below T_c; the latter model was superior in reproducing the line shapes below 2Δ but required modification to agree with the high-frequency results. However, neither model produced satisfactory results below T_c. The unperturbed A_g phonon frequencies and the EMV coupling constants were fitted and found to be in good agreement with *ab initio* calculations and other experimental results in similar TCNQ salts. The electronic parameters, most notably the transfer integral, show an unusual temperature dependence, and may have important implications for charge transport in the TCNQ stacking direction.

We have also investigated the structural phase transition in light of the crystal-field distortion theory by Visser *et al*[3]. For light polarized close to the *b* crystallographic axis on the (110) crystal face, the spectral data are, overall, not in good agreement with the expected band structure shown in Fig. 2. The agreement is good in the high-temperature phase, although the origin of the splitting near 10 000 cm^{-1} is unclear. However, below T_c, several expected low-energy charge-transfer bands are absent, most notably the low-energy excitation at 430 cm^{-1}. In the absence of spectral evidence for low-energy excitation at 430 cm^{-1}, the activation energy for interchain transport would be ≈ 0.25 eV both above and below T_c. Consequently, we do not find conclusive spectral evidence that the unusual transport properties of semiconducting $DMTM(TCNQ)_2$ can be explained in terms of low-energy interchain charge transfer.

ACKNOWLEDGMENTS

The authors would like to thank T. Timusk, M. J. Rice, K. F. Ferris, and V. Železný for useful discussions. This research was supported in part by NSF Grant No. OMR-9101676, the Natural Sciences and Engineering Research Council of Canada, and the Canadian Institute for Advanced Research.

[1]S. Oostra, J. L. de Booer, and P. Lange, J. Phys. (Paris) Colloq. **44**, C3-1387 (1983).
[2]M. Almeida, L. Alcacer, S. Oostra, and J. L. de Boer, Synth. Met. **19**, 445 (1987).
[3]R. J. J. Visser, S. van Smaalen, J. L. de Boer, and A. Vos, Mol. Cryst. Liq. Cryst. **120**, 167 (1985).
[4]R. J. J. Visser, J. L. de Boer, and A. Vos, Acta Crystallogr. C **46**, 864 (1990).
[5]P. Kamminga and B. van Bodegom, Acta. Crystallogr. B **37**, 114 (1981).
[6]V. M. Yartsev and A. Graja, Chem. Phys. **130**, 159 (1989).
[7]V. M. Yartsev and A. Graja, Mater. Sci. **14**, 95 (1988).
[8]F. Rachdi, T. Nunes, M. Ribet, P. Bernier, M. Helme, M. Mehring, and M. Almeida, Phys. Rev. B **45**, 8134 (1992).
[9]G. Zimmer, A. C. Kolbert, F. Rachdi, P. Bernier, M. Almeida, and M. Mehring (unpublished).
[10]G. Zimmer, A. C. Kolbert, F. Rachdi, P. Bernier, M. Almeida, and M. Mehring, Chem. Phys. Lett. **182**, 673 (1991).
[11]C. S. Jacobsen, in *Semiconductors and Semimetals,* edited by E. M. Conwell (Academic, New York, 1985), Vol. 27, Chap. 5.
[12]D. B. Tanner, in *Extended Linear Chain Compounds,* edited by J. S. Miller (Plenum, New York, 1982), Vol. 2, Chap. 5.
[13]V. M. Yartsev and R. Świetlik, in Rev. Solid State Sci. **4**, 69 (1990).
[14]R. Bozio and C. Pecile, in *Spectroscopy of Advanced Materials,* edited by R. J. H. Clark and R. E. Hester (Wiley, Chichester, 1990).
[15]M. J. Rice, V. M. Yartsev, and C. S. Jacobsen, Phys. Rev. B **21**, 3437 (1980).
[16]M. J. Rice, Phys. Rev. Lett. **37**, 36 (1976).
[17]R. Bozio, M. Meneghetti, and C. Pecile, Phys. Rev. B **36**, 7795 (1987).
[18]M. J. Rice, V. M. Yartsev, and C. S. Jacobsen, Phys. Rev. B **24**, 6167 (1981).
[19]V. M. Yartsev and C. S. Jacobsen, Phys. Status Solidi B **145**, K 149 (1988).
[20]R. Świetlik and A. Graja, J. Phys. (Paris) Colloq. **44**, C3-1457 (1983).
[21]M. Almeida and L. Alcácer, J. Cryst. Growth **62**, 183 (1985).
[22]M. Almeida, L. Alcácer, and A. Lindegaared-Andersen, J. Cryst. Growth **72**, 567 (1985).
[23]K. D. Cummings, D. B. Tanner, and J. S. Miller, Phys. Rev. B **24**, 4142 (1981).
[24]F. Wooten, *Optical Properties of Solids* (Academic, New York, 1972).
[25]Y. Iida, Bull, Chem. Soc. Jpn. **42**, 637 (1969).
[26]J. Tanaka, M. Tanaka, T. Kawai, T. Takabe, and O. Maki, Bull. Chem. Soc. Jpn. **49**, 2358 (1976).
[27]A. Girlando and C. Pecile, Spectrochim. Acta. A **29**, 1859 (1975).
[28]R. Bozio, I. Zanon, A. Girlando, and C. Pecile, J. Chem. Soc. Faraday Trans. II **74**, 235 (1978).
[29]J. L. Musfeldt, K. Kamarás, and D. B. Tanner, Phys. Rev. B **45**, 10 197 (1992).
[30]R. Świetlik and A. Graja, J. Phys. (Paris) **44**, 617 (1983).
[31]R. H. Boyd and W. D. Phillips, J. Chem. Phys. **43**, 2927 (1965).
[32]P. S. Flandrois and E. D. Chasseau, Acta. Crystallogr. B **33**, 2744 (1977).
[33]J. Hubbard, Phys. Rev. B **17**, 494 (1978).
[34]R. Bozio, A. Girlando, and C. Pecile, J. Chem. Soc. Faraday Trans. II **71**, 1237 (1975).
[35]N. O. Lipari, M. J. Rice, C. B. Duke, R. Bozio, A. Girlando, and C. Pecile, Int. J. Quantum Chem. **11**, 583 (1977).
[36]A. Painelli, A. Girlando, and C. Pecile, Solid State Commun. **52**, 801 (1984).
[37]C. S. Jacobsen, D. B. Tanner, and K. Bechgaard, Phys. Rev. B **28**, 7019 (1983).
[38]H. J. Schulz, Phys. Rev. B **18**, 5756 (1978).
[39]J. F. Kwak and G. Beni, Phys. Rev. B **13**, 652 (1976).
[40]P. F. Maldague, Phys. Rev. B **16**, 2437 (1977).
[41]C. C. Homes and J. E. Eldridge, Phys. Rev. B **42**, 9522 (1990).
[42]The energy-band rescaling arguments will be presented in more detail in a later publication.
[43]M. J. Rice, L. Pietronero, and P. Brüesch, Solid State Commun. **21**, 757 (1977).
[44]A. Brau, P. Breüsch, J. P. Farges, W. Hinz, and D. Kuse, Phys. Status Solidi B **62**, 615 (1974).
[45]E. B. Wilson, Jr., J. C. Decius, and P. C. Cross, *Molecular Vibrations: The Theory of Infrared and Raman Vibrational Spectra* (Dover, New York, 1955).
[46]F. A. Cotton, *Chemical Applications of Group Theory,* 2nd ed. (Wiley, New York, 1971).